Eur Biophys J (2008) 37:229–234
DOI 10.1007/s00249-007-0198-3

BIOPHYSICS LETTER

Osteonectin-derived peptide increases the modulus of a bone-mimetic nanocomposite

Alireza S. Sarvestani · Xuezhong He · Esmaiel Jabbari

Received: 1 February 2007 / Revised: 21 May 2007 / Accepted: 28 May 2007 / Published online: 4 July 2007

Abstract Many factors contribute to the toughness of bone including the presence of nano-size apatite crystals, a dense network of collagen fibers, and acidic proteins with the ability to link the mineral phase to the gelatinous collagen phase. We investigated the effect of a glutamic acid (negatively charged) peptide (Glu6), which mimics the terminal region of the osteonectin glycoprotein of bone, on the shear modulus of a synthetic hydrogel/apatite nanocomposite. One end of the synthesized peptide was functionalized with an acrylate group (Ac-Glu6) to covalently attach the peptide to the hydrogel phase of the composite matrix. When microapatite crystals (5 μm diameter) were used, addition of Ac-Glu6 peptide did not affect the modulus of the microcomposite. However, when nanoapatite crystals (100 nm diameter) were used, addition of Ac-Glu6 resulted in significant reinforcement of the shear modulus of the nanocomposite (~100% in elastic shear modulus). Furthermore, addition of Ac-Gly6 (a neutral glycine sequence) or Ac-Lys6 (a positively charged sequence) did not reinforce the nanocomposite. These results demonstrate that the reinforcement effect of the Glu6 peptide, a sequence in the terminal region of osteonectin, is modulated by the size of the apatite crystals. The findings of this work can be used to develop advanced biomimetic composites for skeletal tissue regeneration.

Keywords Nanocomposite · Hydrogel · Apatite · Peptide reinforced · Bone

A. S. Sarvestani · X. He · E. Jabbari (✉)
Biomimetic Materials and Tissue Engineering Laboratories, Department of Chemical Engineering, Swearingen Engineering Center, University of South Carolina, Rm 2C11, Columbia, SC 29208, USA
e-mail: jabbari@engr.sc.edu

Introduction

The bone is a composite of collagen, a protein-based gelatinous network, and inorganic apatite crystals (Glimcher 1992). The combination of a hard inorganic material and an elastic hydrogel network provides unique mechanical properties to the bone (Fantner et al. 2004; Athanasiou et al. 2000) and facilitates communication with the cellular environment (Young 2003). The collagen phase gives form to the bone and contributes to its ability to resist bending, while the mineral component resists compression (Bailey and Knott 1999). The unique factors that contribute to the toughness of bone are the presence of nano-size apatite crystals, a dense network of collagen fibers (Young 2003) on which the mineral crystals are deposited (Boskey 1992), and the acidic proteins with the ability to link the calcium-binding apatite crystals to collagen fibers to form a completely crosslinked network (Termine et al. 1981).

The aqueous collagen phase, with a plethora of non-collagenous proteins (NCP), plays a central role in the regulation of mineralization, modulation, and control of cellular functions, maintenance of matrix integrity, and the extent of mineral–collagen interactions (Buckwalter and Cooper 1995; Sikavitsas et al. 2001). One of the NCPs with bone-specific functions is osteonectin or *bone connector*, because it has a strong affinity for both collagen and hydroxyapatite (HA) and it is believed to be a bone-specific nucleator of mineralization (Young 2003; Fujisawa et al. 1996). In the process of cartilage-to-bone transition during fracture repair, one of the key initial events is the switch from osteonectin to osteopontin mRNA in chondrocyte maturation, followed by the expression of mRNAs for osteonectin, osteopontin, and osteocalcin in the ossification front (Nakase et al. 1998; Sodek et al. 2002).

It is believed that the first 17 NH_2-terminal amino acids of osteonectin are responsible for binding to the bone collagen network (Xie and Long 1996), while a glutamic acid-rich sequence binds to the bone HA nanopartilces (Fujisawa et al. 1996). Among all NCPs, osteonectin has the highest affinity for calcium ions.[6] In the presence of osteonectin, a greater supersaturation of inorganic phosphates is required for precipitation of calcium phosphate and formation of HA under physiological conditions (Doi et al. 1992). Furthermore, the apatite formed in the presence of osteonectin has the smallest crystal size (Boskey et al. 2003). These observations suggest that the switch from osteopontin to osteonectin mRNA in osteogenic cells of the ossification front is to limit the size of the apatite crystals and to produce a crosslinked composite by linking the collagen network to the mineral phase.

In this work, we show evidence that a glutamic acid-rich peptide (a sequence of six glutamic acids) derived from osteonectin, functionalized with an acrylate group for covalent attachment to the matrix, significantly increases the shear modulus of a bone-mimetic hydrogel/apatite nanocomposite and improves the dispersion of apatite nanoparticles in aqueous solution. The biodegradable in situ crosslinkable poly(lactide ethylene oxide fumarate) (PLEOF) hydrogel and HA crystals were used to mimic the gelatinous and mineral phases of the bone matrix, respectively.

Materials and methods

The Glu-Glu-Glu-Glu-Glu-Glu peptide sequence (negatively charged) with an acrylate group at one chain-end (Fig. 1), hereafter designated as Ac-Glu6, was synthesized manually in the solid phase in our laboratory on the Rink Amide NovaGel^{TM} resin (He and Jabbari 2006). Briefly, the Fmoc-protected amino acids were coupled to the resin in *N*,*N*-dimethylformamide using *N*,*N*′-diisopropylcarbodiimide and *N*,*N*-dimethylaminopyridine as the coupling agents. After coupling the last amino acid, the Fmoc-protecting group of the last glutamate residue was selectively deprotected with piperidine. One end was acrylated directly on the peptidyl resin by coupling acrylic acid to the amine group of the last glutamine residue in the peptide sequence. The resin was treated with 95% TFA/2.5% TIPS/2.5% water for 2 h to cleave the peptide from the resin. The solution was precipitated in ether, the solid was purified by preparative HPLC (Waters, Milford, MA, USA), and the product was freeze-dried. The product was characterized by mass spectrometry with a Finnigan 4500 spectrometer (He and Jabbari 2006). A similar procedure was used to synthesize the neutral Gly-Gly-Gly-Gly-Gly-Gly (Gly6) peptide and positively charged Lys-Lys-Lys-Lys-Lys-Lys (Lys6) peptide sequences with an acrylate group at one chain-end (Ac-Gly6 and Ac-Lys6, respectively).

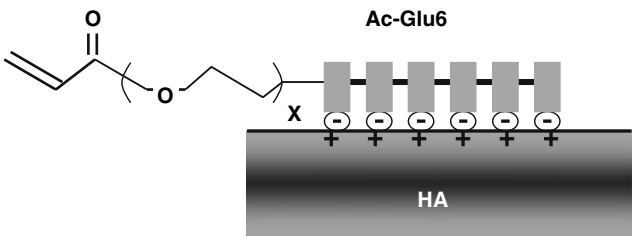

Fig. 1 Schematic diagram to illustrate the ionic interaction between Ac-Glu6 peptide and HA nanoparticle. Terminal acrylate group of the Ac-Glu6 provides an unsaturated group for covalent crosslinking of the peptide to the PLEOF matrix, while Glu6 provides a sequence for physical attachment to HA nanoparticles

A total of 100 mg Ac-Glu6 peptide (M_n = 900 Da) was dissolved in 0.825 ml of distilled deionized water by vortexing and heating the mixture to 50°C. HA fillers (~100 nm; Berkeley Advanced Biomaterials, Berkeley, CA, USA) with loadings from 3 to 9% by volume of the final mixture, corresponding to 10–30 wt% (ρ_{HA} = 3.16 g/cm^3) were added to the PLEOF polymerizing mixture and the resulting dispersion was sonicated for 5 min. Larger spherical particles, with average diameter of 5 μm, were also used to investigate the effect of particle size.

Poly(lactide ethylene oxide fumarate, a novel in-situ crosslinkable terpolymer with excellent biocompatibility, consists of ultra low molecular weight poly(L-lactide) (ULMW PLA) and poly(ethylene glycol) (PEG) blocks linked by fumaric acid. The water content of the hydrogel can be controlled by the ratio of the hydrophobic PLA to hydrophilic PEG blocks in the macromer. ULMW PLA, with M_n in the range of 1–2 kDa, was synthesized by ring opening polymerization of the L-lactide monomer. PLEOF was synthesized by condensation polymerization of ULMW PLA and PEG with fumaryl chloride (FuCl) (Jabbari and He 2006). The molar ratio of FuCl:PEG was 0.9:1.0 and the weight ratio of PEG to ULMW PLA was 70:30 to produce a hydrophilic water-soluble terpolymer. The structure of the PLEOF macromer was characterized by ^{1}H-NMR and FTIR (Sarvestani and Jabbari 2006). The PLEOF macromer with PLA and PEG molecular weights of 1.2 kDa (PI of 1.1) and 3.4 kDa (PI of 1.1) had M_n and PI of 10.5 kDa and 1.7, respectively, as determined by GPC.

The composite mixture was prepared by dispersing the HA/Ac-Glu6 in PLEOF macromer (0.04 M) and methylene bisacrylamide crosslinker (0.25 M). The neutral redox initiation system with equimolar concentrations (0.03 M) of ammonium persulfate and tetramethylethylenediamine was used to maintain the pH of the polymerizing mixture constant at 7.4. The mixture was mixed vigorously for 20 s,

injected between the parallel plates of the rheometer, and the gelation kinetics measured by rheometry. The dynamic storage modulus (G') was measured at 37°C by a TA instrument AR2000 rheometer equipped with a parallel plate geometry (diameter: 20 mm). The time sweep oscillatory shear measurements were done at a constant frequency of 1 Hz for 3 h. The deformation amplitude in time sweep measurements was 1% to remain within the linear region of viscoelasticity.

Results

Figure 2 shows the time dependence of G', the storage shear modulus of the hydrogel/nanoapatite composite, during the course of gelation. The shear modulus of the samples with Ac-Glu6 linker was higher than those without the peptide linker, at the same volume fraction. The enhancement in stiffness was more pronounced for the samples with higher filler concentration. Figure 3 shows the dependence of the shear modulus of the composites on the size of the dispersed HA particles. Nanoapatite composites (treated and untreated) displayed far larger stiffness compared to microcomposites, at the same volume fraction. The modulus of the composites with micron size particles did not appreciably change with the addition of Ac-Glu6.

For low HA volume fractions, the contribution of hydrodynamic effect to the modulus of the composite is modeled by Guth–Smallwood equation, which for spherical particles is given by (Guth 1945)

$$G'_0(\Phi) = G'_0(0)(1 + 2.5\,\Phi) \quad (1)$$

Here, $G'_0(0)$ and $G'_0(\Phi)$ are the low amplitude storage modulus of the neat polymer and that of the composite, respectively, and Φ represents the volume fraction of the dispersed particles. The storage modulus of the composites prepared with micron size particles can be reasonably predicted by Eq. 1, as shown in Fig. 3. However, the large difference between the experimental results and the predictions of Eq. 1 for composites prepared with nano-size HA implies that the reinforcement cannot be explained solely by the hydrodynamic effect in these systems.

Hydroxyapatite nanoparticles tend to agglomerate and form larger structures as a result of the inter-particle electrostatic or van der Waals' interactions (Sarvestani and Jabbari 2006). In addition, PLEOF chains interact by strong ionic interactions with the surface of HA particles through Ac-Glu6 linkers. Untreated HA nanoparticles interact with PLEOF chains between crosslink points by relatively weaker dipolar interactions (compared to Ac-Glu6 ionic interaction). The relative magnitude of these two competitive processes, i.e., HA–HA and PLEOF–HA interactions, determines the reinforcement mechanism and evolution of the composite properties during deformation.

To provide further evidence for energetic affinity between the Ac-Glu6 peptide and HA and its effect on the shear modulus of the nanocomposites, similar measurements were performed on the PLEOF/HA composites treated with equal molar concentrations of Ac-Gly6 and Ac-Lys6 in place of Ac-Glu6. Contrary to the Glu6 peptide, Gly6, and Lys6 are neutral and positively charged, respectively. HA/Ac-Gly6 and HA/Ac-Lys6 nanocomposites with 9 vol% apatite did not show a significant change

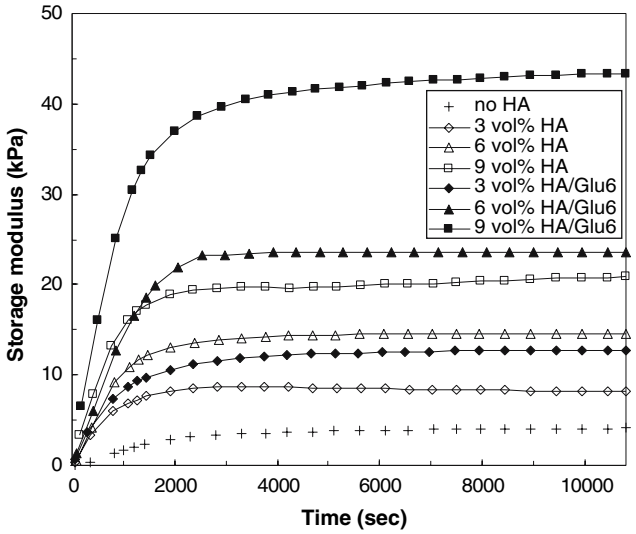

Fig. 2 Evolution of viscoelastic properties of the hydrogel/apatite composites with gelation time. The storage modulus of the untreated and Ac-Glu6 treated samples composites are designated by HA and HA/Glu6, respectively

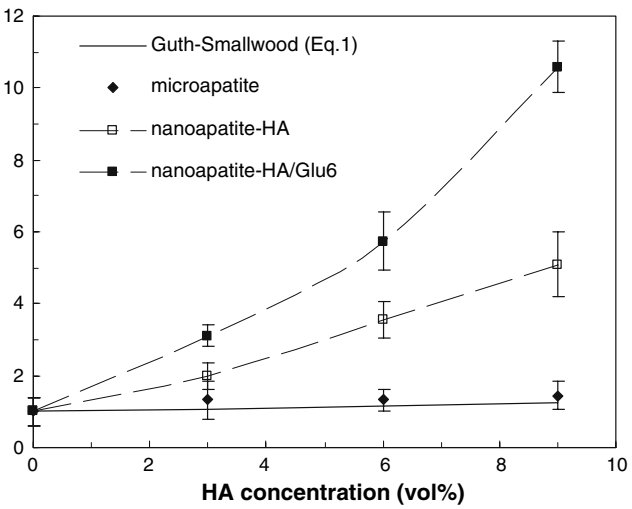

Fig. 3 Comparison of the experimentally determined normalized shear modulus of the composites with the predictions of Guth–Smallwood equation

in storage shear modulus compared to that without HA surface treatment, as shown in Fig. 4. The Ac-Lys6 is a positively charged sequence and it is expected to interact with the phosphate groups on the apatite surface in the same way that the negatively charged Ac-Glu6 sequence interacts with calcium ions, but the results in Fig. 4 do not support this expectation. The charge ratio of Ca^{2+} to PO_4^{3-} groups in the HA crystal, with atomic composition $[Ca_{10}(PO_4)_6(OH)_2]$, is greater than 1 and, to meet the requirement for electro-neutrality, the negatively charged OH^- groups compensate for the imbalance (De Leeuw 2004). Electronic structure and interatomic potential-based calculations show that the OH^- groups, in the bulk as well as the HA surface, are easily replaced by negatively charged fluoride ions (De Leeuw 2004). Furthermore, phosphate and fluoride ions have been demonstrated to alter the mineral–organic interactions and influence the mechanical properties of bone (Walsh and Guzelsu 1994). It is well established that certain small anionic molecules and polymers like poly(vinyl phosphonic acid) (Choi et al. 2006) and poly(acrylamide-co-acrylic acid) (Pearce 1981) displace negatively charged hydroxyl groups (and in some cases phosphate groups) to interact and bond with calcium ions on the apatite surface. Based on these previous results, we believe that the Ac-Glu6 sequence ionically interacts with the apatite crystals by replacing the weakly bound hydroxyl groups (and perhaps the surface bound phosphate groups) from the surface, but the same mode of interaction is not energetically favorable for Ac-Lys6; that is Ac-Lys6 cannot replace the positively charged surface calcium ions to interact with the apatite crystals. These results demonstrate that the increase in adsorption energy and its effect on the overall viscoelastic response of the nanocomposite is specific to the Ac-Glu6 peptide, and the reinforcement is amplified as the size of the nanoparticles is reduced from 5 μm to 100 nm.

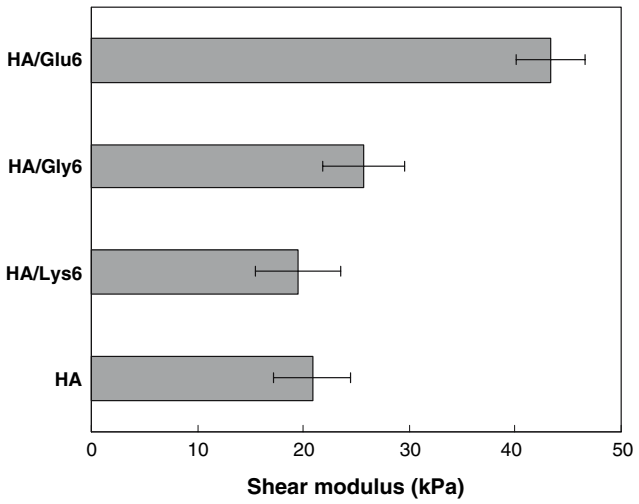

Fig. 4 Comparison of shear modulus of the PLEOF/HA composites with 9 vol% untreated nanoparticles with nanoparticles treated with Ac-Glu6, Ac-Gly6, and Ac-Lys6

A PLEOF segment between two consecutive crosslink points can attach to HA nanoparticles by ionic interactions, hydrogen bonding, or other energetic interactions forming loops, tails, or sequences of bound monomers. The ionic bonds formed by the interaction of Ac-Glu6 with HA have a relatively higher adsorption energy (compared to polar interactions in the absence of Ac-Glu6) and longer residence time on the HA particles. Thus, more HA–PLEOF bonds are expected to exist in surface treated samples at any instant of time compared to untreated samples. This gives rise to a higher concentration of (physical) PLEOF–HA crosslinks, which according to the theory of rubber elasticity (Maier and Göritz 1996), leads to higher modulus of the HA/Ac-Glu6 composites. This does not imply that the presence of HA surface favors crosslinking in the polymer, but the ionic interactions with the surface count as additional physical crosslinks. On the other hand, lower storage modulus of untreated samples indicate a weaker polymer–filler interaction and a stronger tendency for HA particles to aggregate (Heinrich and Klüppel 2002).

The TEM micrographs of HA dispersions in untreated and Ac-Glu6 treated samples, in Fig. 5, support these conclusions. These micrographs demonstrate that treatment of HA nanoparticles with the Ac-Glu6 peptide gave rise to a more homogeneous microstructure of small aggregates or individual HA nanoparticles. This effect can be attributed to the steric hindrance of strongly adsorbed peptide linkers and the stabilization of the HA particles against fusion. This provides more surface area for interaction of PLEOF chains with HA nanoparticles. These results demonstrate that one of the factors contributing to the toughness of bone is the crosslinking of the bone's gelatinous phase (simulated with the PLEOF hydrogel) and mineral phase (simulated by HA

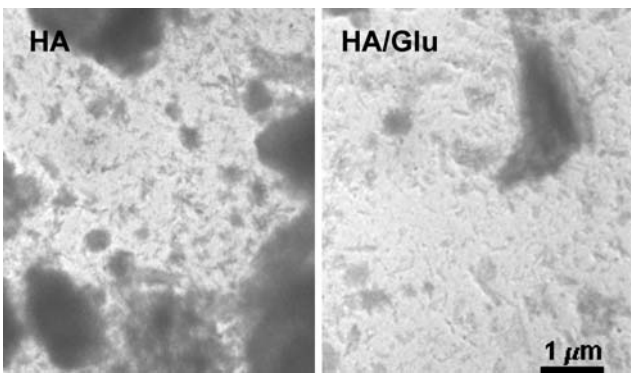

Fig. 5 TEM images of sonicated PLEOF/HA nanocomposites with untreated (*left*) and Ac-Glu6 treated (*right*) HA nanoparticles

nanoparticles) by a specific peptide sequence derived from osteonectin (simulated by Ac-Glu6 with an acrylate group for attachment to the PLEOF network and the Glu6 peptide for bonding to HA particles).

We emphasize that the ionic bonding between the glutamic acid sequence of osteonectin and the HA surface is one of many specific interactions at the matrix/mineral interface that contribute to the structural stability and mechanical strength of the natural bone. Specific sequences on proteoglycans (Raspanti et al. 2000), collagen fibrils, and non-collagenous bone matrix proteins (Ferris et al. 1987; Robey et al. 1993; Young 2003), like osteopontin (McKee and Nanci 1996) and osteocalcin (Hoang et al. 2003), are believed to contribute to bonding the organic matrix to apatite crystals. For example, it was suggested recently that calcium-mediated sacrificial bonds between the non-collagenous matrix components act as a glue to hold the mineralized fibrils together (Fantner et al. 2005, 2006). In addition, Fourier transform infrared microscopy studies of human cortical bone before and after X-ray radiation have shown that side chain carboxylate groups of the collagen matrix are involved in coordination with the apatite bound calcium ions, and these interactions are removed by decarboxylation upon irradiation (Hubner et al. 2005).

Conclusion

The effect of a glutamic acid sequence (Glu6) on the viscoelastic response of a hydrogel reinforced with HA particles was studied. The peptide mimics the terminal region of the osteonectin glycoprotein of bone, which has ionic interactions with HA. Size and surface treatment of HA particles with Glu6 were found to be the primary factors affecting the stiffness of the composites. While surface treatment of microparticles (5 (m) showed no sensible effect on the shear modulus of the hydrogel/HA composites, the stiffness of the composites prepared with nanoapatite (~100 nm) improved significantly after treatment with Glu6, particularly at higher HA volume fractions. This behavior was attributed to the increase in the density of transient crosslinks due to Glu6–HA strong ionic interactions and stabilization of nanoparticles against fusion. The findings of this work can be used to develop advanced biomimetic nanocomposites for skeletal tissue regeneration.

Acknowledgments This work was supported by grants from the AO (Arbeitsgemeinschaft Fur Osteosynthesefragen) Foundation, the Aircast Foundation, the Office of Research and Health Sciences at the University of South Carolina (USC), and the USC NanoCenter.

References

Athanasiou KA, Zhu CF, Lanctot DR, Agrawal CM, Wang X (2000) Fundamentals of biomechanics in tissue engineering of bone. Tissue Eng 6:361–381

Bailey AJ, Knott L (1999) Molecular changes in bone collagen in osteoporosis and osteoarthritis in the elderly. Exp Gerontol 34:337–351

Boskey AL (1992) Mineral–matrix interactions in bone and cartilage. Clinical orthopedics and related research. Clin Orthop Relat Res 281:244–274

Boskey AL, Moore DJ, Amling M, Canalis E, Delany AM (2003) Infrared analysis of the mineral and matrix in bones of osteonectin-null mice and their wildtype controls. J Bone Miner Res 8:1005–1011

Buckwalter JA, Cooper RR (1995) Bone biology: part II: formation, form, modeling, remodeling, and regulation of cell function. J Bone Joint Surg 77A:1276–1289

Choi HW, Lee HJAE, Kim KJ, Hyun-Min K, Lee SC (2006) Surface modification of hydroxyapatite nanocrystals by grafting polymers containing phosphonic acid groups. J Colloid Interface Sci 304:277–281

De Leeuw NH (2004) A computer modelling study of the uptake and segregation of fluoride ions at the hydrated hydroxyapatite (0001) surface: introducing a Ca[10](PO[4])[6](OH)[2] potential model. Phys Chem Chem Phys 6:1860–1866

Doi Y, Horiguchi T, Kim SH, Moriwaki Y, Wakamatsu N, Adachi M, Ibaraki K, Moriyama K, Sasaki S, Shimokawa H (1992) Effects of non-collagenous proteins on the formation of apatite in calcium beta-glycerophosphate solutions. Arch Oral Biol 37:15–21

Fantner GE, Birkedal H, Kindt JH, Hassenkam T, Weaver JC, Cutroni JA, Bosma BL, Bawazer L, Finch MM, Cidade GA, Morse DE, Stucky GD, Hansma PK (2004) Influence of the degradation of the organic matrix on the microscopic fracture behavior of trabecular bone. Bone 35:1013–1022

Fantner GE, Hassenkam T, Kindt JH, Weaver JC, Birkedal H, Pechenik L, Cutroni JA, Cidade GAG, Stucky GD, Morse DE, Hansma PK (2005) Sacrificial bonds and hidden length dissipate energy as mineralized fibrils separate during bone fracture. Nat Mater 4:612–616

Fantner GE, Oroudjev E, Schitter G, Golde LS, Thurner P, Finch MM, Turner P, Gutsmann T, Morse DE, Hansma H, Hansma PK (2006) Sacrificial bonds and hidden length: unraveling molecular mesostructures in tough materials. Biophys J 90:1411–1418

Ferris BD, Klenerman L, Dodds RA, Bitensky L, Chayen J (1987) Altered organization of noncollagenous bone-matrix in osteoporosis. Bone 8:285–288

Fujisawa R, Wada Y, Nodasaka Y, Kuboki Y (1996) Acidic amino acid-rich sequences as binding sites of osteonectin to hydroxyapatite crystals. Biochim Biophys Acta 1292:53–60

Glimcher MJ (1992) The nature of the mineral component of bone and the mechanism of calcification. In: Coe FL, Favus MJ (eds) Disorders of bone and mineral metabolism. Raven Press, New York, pp 265–286

Guth EJ (1945) Theory of filler reinforcement. J Appl Phys 16:20–25

He X, Jabbari E (2006) Solid-phase synthesis of reactive peptide crosslinker by selective deprotection. Protein Pept Lett 13:715–718

Heinrich G, Klüppel M (2002) Recent advances in the theory of filler networking in elastomers. Adv Polym Sci 160:1–44

Hoang QQ, Sicheri F, Howard AJ, Yang DSC (2003) Bone recognition mechanism of porcine osteocalcin from crystal structure. Nature 425:977–980

Hubner W, Blume A, Pushnjakova R, Dekhtyar Y, Hein HJ (2005) The influence of X-ray radiation on the mineral/organic matrix interaction of bone tissue: an FT-IR microscopic investigation. Int J Artif Organs 28:66–73

Jabbari E, He X (2006) Synthesis and material properties of functionalized lactide oligomers as in situ crosslinkable scaffolds for tissue regeneration. Polymer Prepr 47:353–354

Maier PG, Göritz D (1996) Molecular interpretation on the Payne effect. Kautsch Gummi Kunstst 49:18–21

McKee MD, Nanci A (1996) Osteopontin at mineralized tissue interfaces in bone, teeth, and osseointegrated implants: ultrastructural distribution and implications for mineralized tissue formation, turnover, and repair. Microsc Res Tech 33:141–164

Nakase T, Sugimoto M, Sato M, Kaneko M, Tomita T, Sugamoto K, Nomura S, Kitamura Y, Yoshikawa H, Yasui N, Yonenobu K, Ochi T (1998) Switch of osteonectin and osteopontin mRNA expression in the process of cartilage-to-bone transition during fracture repair. Acta Histochem 100:287–295

Pearce EIF (1981) Ion displacement following the adsorption of anionic macromolecules on hydroxyapatite. Calcif Tissue Int 33:395–402

Raspanti M, Congiu T, Alessandrini A, Gobbi P, Ruggeri A (2000) Different patterns of collagen–proteoglycan interaction: a scanning electron microscopy and atomic force microscopy study. Eur J Histochem 44:335–343

Robey PG, Fedarko NS, Hefferan TE, Bianco P, Vetter UK, Grzesik W, Friedenstein A, Van der Pluijm G, Mintz KP, Young MF, Kerr JM, Ibaraki K, Heegaard AM (1993) Structure and molecular regulation of bone-matrix proteins. J Bone Miner Res 8:S483–S487

Sarvestani AS, Jabbari E (2006) Modeling and experimental investigation of rheological properties of injectable poly(lactide ethylene oxide fumarate)/hydroxyapatite nanocomposites. Biomacromolecules 7:1573–1580

Sikavitsas VI, Temenoff JS, Mikos AG (2001) Biomaterials and bone mechanotransduction. Biomaterials 22:2581–2593

Sodek J, Zhu B, Huynh MH, Brown TJ, Ringuette M (2002) Novel functions of the matricellular proteins osteopontin and osteonectin. Connect Tissue Res 43:308–319

Termine JD, Kleinman HK, Whitson SW, Conn KM, McGarvey ML, Martin GR (1981) Osteonectin, a bone-specific protein linking mineral to collagen. Cell 26:99–105

Walsh WR, Guzelsu N (1994) Compressive properties of cortical bone: mineral-organic interfacial bonding. Biomaterials 15:137–145

Xie R-L, Long GL (1996) Elements within the first 17 amino acids of human osteonectin are responsible for binding to type V collagen. J Biol Chem 271:8121–8125

Young MF (2003) Bone matrix proteins: their function, regulation, and relationship to osteoporosis. Osteoporos Int 14(Suppl 3):S35–S42